Chemical Engineering Science 329 (2026) 123782

Contents lists available at ScienceDirect

Chemical Engineering Science

journal homepage: www.elsevier.com/locate/ces

Pressurized CO_2 electrochemical conversion into formate using an undivided cell equipped with large-area Sn electrodes

Pengfei Ma [a,1,2], Xinya Wang [a,1,2], Federica Proietto [b], Xianming Zhang [a,*], Onofrio Scialdone [b,*]

[a] College of Chemistry and Chemical Engineering, Taiyuan University of Technology, No.79 West Yingze Street, 030024 Taiyuan, Shanxi, China
[b] Dipartimento di Ingegneria, Università degli Studi di Palermo, Viale delle Scienze, 90128 Palermo, Italy

ARTICLE INFO

Keywords:
Electrochemical CO_2 reduction
Formate
High current
Undivided cell
CO_2 pressure

ABSTRACT

Recently, the pressurized electrochemical reduction of CO_2 ($PrCO_2RR$) in aqueous systems has emerged as a particularly promising route for the conversion of CO_2 into value-added products. To facilitate the development of this process at an applicative scale, it is essential to evaluate its performance at appreciable current intensities (I) using systems that are low-cost and easily scalable.

In this work, the $PrCO_2RR$ to formate (FA) was carried out in a simple undivided cell equipped with relatively large-area Sn cathode, investigating the effects of several key parameters, including I (4–20 A), CO_2 pressure (P_{CO_2}, 1–30 bar), supporting electrolyte concentration, and electrolysis duration. The best performances were obtained at intermediate values of both I and P_{CO_2}, enabling efficient CO_2 conversion to FA with high productivity and final formate concentrations up to 5 wt%, which are significantly higher than those previously reported in the literature for $PrCO_2RR$.

1. Introduction

To curb the human-induced carbon emissions, the CO_2 transformation into useful products has become a focal point of research (Bushuyev et al., 2018). Among the various CO_2 valorisation pathways, the electrochemical reduction of CO_2 (CO_2RR) stands out as a particularly promising route due to notable benefits, including its ability to operate under relatively mild conditions, the potential for compact and modular system configurations and its integration and compatibility with intermittent renewable energy inputs (Proietto et al., 2021). CO_2RR can yield more valuable products, such as formic acid or formate (FA) (Proietto et al., 2021; Philips et al., 2020), syngas (Bushuyev et al., 2018; Yaashikaa et al., 2019; Tang et al., 2021), carbon monoxide (CO) (Masel et al., 2021; Zhang et al., 2024; Yang et al., 2023; Proietto et al., 2022), methane, and various hydrocarbons (Proietto et al., 2021; Leonzio et al., 2024; Qiu et al., 2023) using only CO_2, water and electricity ideally sourced from renewables. Recently, extensive research has been focused on advancing electrochemical strategies for CO_2RR; among these, the pressurized cathodic reduction of CO_2 ($PrCO_2RR$) in aqueous systems has emerged as a particularly promising pathway for valorising CO_2. A wide range of cathodes has been studied for $PrCO_2RR$, including Ag (Proietto et al., 2024; Dufek et al., 2012; Gabardo et al., 2018; Proietto et al., 2021), Sn (Proietto et al., 2023; Scialdone et al., 2016; Proietto et al., 2018; Ramdin et al., 2019; Morrison et al., 2019; Proietto et al., 2025), Bi (Proietto et al., 2025; Proietto et al., 2023; Sun et al., 2025; Ruan et al., 2022; He et al., 2018) Pb (Todoroki et al., 1995; Köleli and Balun, 2004; Mizuno et al., 1995), Hg and In (Todoroki et al., 1995; Mizuno et al., 1995), Cu (Qiu et al., 2023; Hara et al., 1994; Girichandran et al., 2024; Zong et al., 2023; Li et al., 2020), Ni (Yaashikaa et al., 2019; Proietto et al., 2025; Kudo et al., 1993), and Au (Morrison et al., 2023; Hara et al., 1995), among others (Hara et al., 1995; Chen et al., 2024). Recent economic analyses have highlighted FA and CO as the particularly attractive outputs of $PrCO_2RR$, with promising prospects for achieving profitability (Proietto et al., 2025; Proietto et al., 2021; Huang et al., 2021). Despite these promising features, the crucial hurdles to ensure the economically viable production for large-scale application are to ensure high productivity (i.e., operation at high current intensity – I), high selectivity and faradaic efficiency (EF), as well as long-term

* Corresponding authors.
E-mail addresses: zhangxianming@tyut.edu.cn (X. Zhang), onofrio.scialdone@unipa.it (O. Scialdone).
[1] Co-first author, these authors contributed equally.
[2] Pengfei Ma and Xinya Wang are co-first authors.

https://doi.org/10.1016/j.ces.2026.123782
Received 13 January 2026; Received in revised form 27 February 2026; Accepted 12 March 2026
Available online 13 March 2026

stability and low capital costs. It is worth to mention that the low CO_2 solubility in water-based electrolyte at 1 bar (~33 mM in water at 25 °C) results in severe mass transport limitations, restricting the maximum achievable current density (*j*) and *I*, and poor space–time yields. $PrCO_2RR$ can enhance the product productivity (high *j* and *I*) and the target product selectivity, reduce the energy consumption and avoid the use of expensive electrodes such as gas diffusion ones. In water-based electrolytes, CO_2 solubility rises with increasing its partial pressure (P_{CO_2}). Several studies have highlighted that $PrCO_2RR$ can accelerate the CO_2 mass transport, thereby enabling operation at higher *j* and *I* and faster FA or CO production while minimising the H_2 evolution reaction to improve CO_2RR selectivity (Proietto et al., 2025; Huang et al., 2013). Recent studies have highlighted the importance to reduce overall costs of the process (Proietto et al., 2024; Proietto et al., 2023; Scialdone et al., 199 (2016); Proietto et al., 2018; Ramdin et al., 2019; Proietto et al., 2025). This includes also the potential use of less expensive equipment (e.g., undivided cells, low-cost cathodes). While high-pressure systems can lead to increased capital and operational expenditures, moderate pressures (up to about 20 bar) generally do not impose significant cost penalties (Qiu et al., 2023; Proietto et al., 2021). For instance, Proietto et al. (Proietto et al., 2024; Proietto et al., 2025) reported that the identification of proper conditions, in terms of P_{CO_2} and *j*, can allow to minimize both capital and operational costs as well as energy consumption using different cathodes. Recent findings also show that P_{CO_2} plays a crucial role in determining reaction selectivity. Higher P_{CO_2} levels lead to increased CO_2 surface coverage and reduced proton concentration at the cathode, favouring CO_2 reduction over H_2 generation (Todoroki et al., 1995; Mizuno et al., 1995; Hussain et al., 2025; Lamaison et al., 2020; Heuser et al., 2025). However, even if some interesting scale-up were recently reported for CO_2RR (as an example, Izadi et al. used electrodes with a surface of 400 cm^2 (Izadi et al., 2026), most of studies performed at elevated pressure, mainly using divided cells, operated at relatively high *j* but with small electrode areas and consequently with small *I*, thus giving rise to very slow production of FA and/or CO and low final FA concentrations (Hussain et al., 2025; Lamaison et al., 2020; Heuser et al., 2025).

The final FA concentration ([FA]) is of particular importance because the electrolysis step is followed by a concentration stage that strongly influences the overall process economics: the lower the [FA] obtained during electrolysis, the higher the costs associated with the overall process (Proietto et al., 2021). Proietto et al. (Proietto et al., 2018), employing an undivided filter-press cell with a Sn plate cathode (active area: 9 cm^2), achieved 1.26 wt% FA (273 mM) with a FE of ~ 82% at 23 bar and 0.45 A. Similarly, Ramdin et al. (Ramdin et al., 2019) reported $PrCO_2RR$ at 50 bar using a larger electrode area (80 cm^2), obtaining a final FA concentration of 1 wt% (217 mM) with a ~ 90% FE after 20 min of electrolysis at 2.4 A in a divided electrochemical cell equipped with a Sn cathode and a bipolar membrane. Sun et al. (Sun et al., 2025) observed an increase in *I* from approximately 0.5 A (≈2000 mA mg^{-1}) to 1.7 A (7084 mA mg^{-1}) when pressurizing CO_2 from 1 to 40 bar, achieving a FE of 78% using a 0.5 cm^2 two-dimensional Bi_2O_2Se electrode (0.5 mg cm^{-2}) in a CO_2-saturated 0.5 M $KHCO_3$ electrolyte. Although these studies demonstrate the benefits of pressurization, they generally operate with small electrode areas and consequently with low *Is*, limiting FA production rates and the final [FA]. Therefore, a systematic investigation of $PrCO_2RR$ under conditions combining high productivity of FA (i.e., high *I*), large electrode area and pressurization, with a specific focus on achieving high FA concentrations, is still lacking.

To address these gaps, the present study conducts a comprehensive evaluation of $PrCO_2RR$ to FA over a wide range of operating conditions. A simple undivided cell equipped with a low-cost Sn plate cathode was employed to assess the feasibility of using an apparatus characterized by a small capital investment. The combined effects of P_{CO_2} (1–30 bar) and industrially more relevant *Is* (4.5–20 A) were explored using a relatively large-area cathode (260 cm^2). The effects of the concentration of the supporting electrolyte and of the duration of the electrolysis were also evaluated. Process performance was assessed in terms of formate concentration ([FA]), faradaic efficiency (FE), productivity, and energy consumption.

2. Materials and methods

2.1. Electrochemical CO_2 reduction system

The electrochemical cell employed a two-electrode, parallel plate configuration with a surface of electrodes of 260 cm^2. The cathode was a tin sheet (Sn foil, RPE, 99% purity). The anode was a commercial Dimensionally Stable Anode (DSA) composed of a titanium substrate coated with a mixed metal oxide layer of iridium and tantalum ($Ti/IrO_2 - Ta_2O_5$), sourced from UTron Technology Co., Ltd. Prior to its installation in the reactor, the DSA anode was cleaned in an ultrasonic bath containing deionized water to ensure a clean and active surface. A rigorous and multi-step pre-treatment protocol was implemented for the tin cathode before each experimental run, consisting of three sequential steps: i) chemical etching (the tin foil was immersed in an 11% aqueous HNO_3 solution for 2 min) ii) mechanical smoothing and iii) ultrasonic cleaning. The experiments were conducted in a custom-built, continuous recirculation reaction system designed for operation under pressure, moving beyond typical lab-scale batch configurations to better simulate process-oriented conditions. The core of the system was a pressurized, undivided filter-press electrochemical cell featuring the parallel plate electrodes described in Fig. 1, with a fixed inter-electrode gap of 0.5 cm.

The process flow diagram is shown in Fig. 2. The electrolyte was continuously circulated through the system using a centrifugal pump (VIKDA-V24) with a maximum delivery capacity of 300 mL min^{-1}. The main storage tank is constructed of stainless steel and features two ports at its top: one port branches into two lines, one for carbon dioxide feed and the other for liquid phase circulation; the other port is used for venting gaseous products. All system components, including tubing and connectors, were fabricated from AISI 316 stainless steel to ensure chemical inertness and corrosion resistance. The total volume of the closed-loop system exceeded 1 L. For precise control of the operating conditions, the system was equipped with a pressure gauge and a pressure relief valve, allowing for regulation of the internal CO_2 pressure. This pressurized design is a key feature, as it significantly increases the solubility of CO_2 in the $NaHCO_3$ aqueous electrolyte according to a relationship that combines Henry's law with the Setschenow equation for electrolyte effects (Han et al., 2011) thereby mitigating mass transport limitations of the reactant to the cathode surface and enabling operation at higher *j*. The combined Henry-Setschenow take in consideration that electrolyte-induced salting-out reduces CO_2 solubility (Han et al., 2011).

For each experiment, the system was charged with a total volume of 0.4 L of the $NaHCO_3$ electrolyte (0.1,0.2,0.5 and 0.8 M). The electrolyte was circulated through the electrochemical cell at a constant flow rate of 56 mL min^{-1}. Simultaneously, CO_2 gas was fed into system to the target initial pressure. All electrolytic experiments were conducted at room temperature under constant current conditions (15, 17.3, 30, 50 mA cm^{-2}). The applied *j* was calculated by normalizing the total current by the geometric surface area of the tin cathode that was wetted and directly exposed to the anode, which was specified as 260 cm^2. To ensure the reliability of the obtained data, each experimental condition was tested in at least two independent runs, and the results were accepted only if the reproducibility was within a 5% margin. Upon completion of each experiment, the entire system was thoroughly cleaned by continuously circulating distilled water to prevent cross-contamination between runs.

2.2. Chemicals and analytical methods

The preparation method for the electrolyte involves dissolving sodium bicarbonate ($NaHCO_3$) in deionized water at concentrations of 0.1,

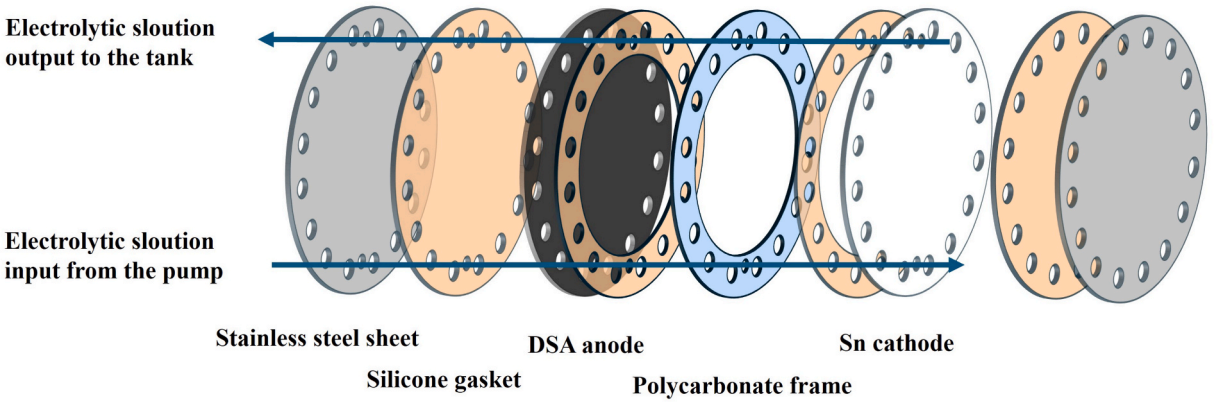

Fig. 1. Schematic view of the electrochemical cell.

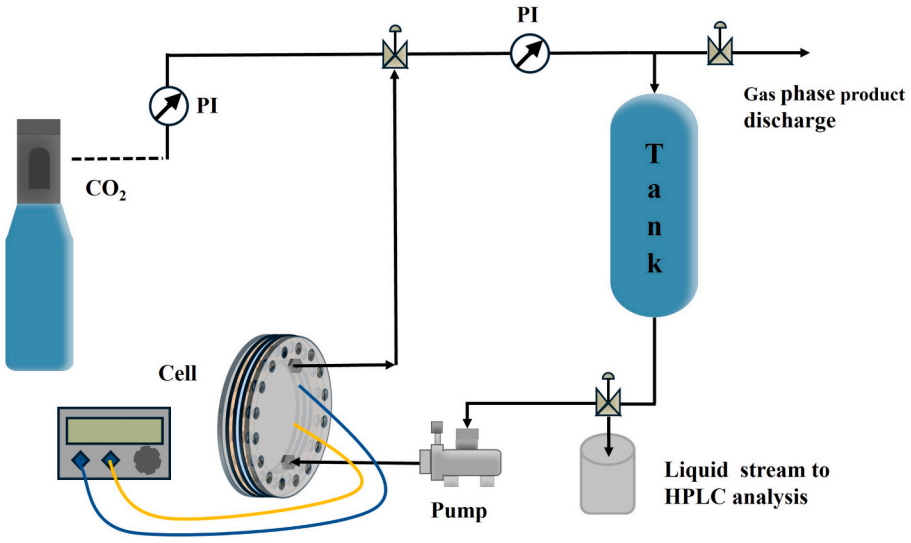

Fig. 2. The process flow diagram of the system.

0.2, 0.5 and 0.8 mol L^{-1}. High-purity carbon dioxide (CO_2, 99.999% purity) was used as the reactant feedstock for all electrolysis experiments. The chemical pre-treatment of the cathode involved an 11% aqueous solution of nitric acid (HNO_3). The concentration of formic acid produced in the liquid phase was quantified using a Shimadzu LC-2060C High-Performance Liquid Chromatography (HPLC) system. The analysis was performed on a C18 column maintained at a constant temperature of 30 °C. The eluting formic acid was detected by a UV–Vis detector set to a wavelength of 210 nm. The mobile phase was a 0.02 M aqueous solution of H_3PO_4, which was eluted at a constant flow rate of 0.6 mL min^{-1}. Quantitative determination of FA concentration was achieved through an external calibration curve generated from standards of known concentration prepared from pure FA.

The performance of the electrochemical process was evaluated by calculating the Faradaic Efficiency (FE) for FA production. The overall FE at a given time t was calculated using equation (1):

$$FE = 2\,F\,V\,[FA]_t / I\,t \quad (1)$$

where F is the Faraday constant (96487C mol^{-1}), V is the total volume of the liquid electrolyte (0.4 L), $[FA]_t$ is the molar concentration of FA at time t, and I is the total applied current. The factor of 2 in the numerator accounts for the two moles of electrons required to reduce one mole of CO_2 to formic acid (eq. (2)).

$$CO2 + 2H+ + 2e- \rightarrow HCOOH \quad (2)$$

The performance of the process was also evaluated in terms of: *i*) energy consumption (EC), Eq. (3), expressed in kWh per mole of formate produced, and *ii*) productivity (r_{FA}), Eq. (4), defined as the mass of FA generated per hour (g h^{-1}) (where MW_{FA} is the molecular weigth of FA 46 g mol^{-1}).

$$EC = \Delta VIt/mol_{FA}[\,=]kWhmol_{FA}^{-1} \quad (3)$$

$$rFA = EFjMW_{FA}/nF[\,=]gh^{-1} \quad (4)$$

3. Results and discussion

3.1. Effect of pressure

As mentioned in the introduction, the performance of CO_2RR at various cathodes can be strongly improved enhancing the P_{CO_2}. In this work, the effect of P_{CO_2} was investigated for the CO_2RR to FA using a tin cathode by performing a series of 3-hour electrolyses in an undivided pressurized cell containing a 0.5 M $NaHCO_3$ solution, under galvanostatic conditions at a *I* of 4.5 A (j = 0.17 kA m^{-2}). The P_{CO_2} values were set at 1, 5, 7, 9, 15 and 20 bar. A Ti/IrO_2–Ta_2O_5 anode was selected because it is known to favour oxygen evolution over FA oxidation to CO_2 (Scialdone et al., 199 (2016)). At 1 bar, the electrolysis yielded a final [FA] of approximately 0.25 M, corresponding to a FA productivity (r_{FA}) of about 1.6 g h^{-1} and an energy consumption (EC) of ~ 0.54 kWh mol^{-1}. The EC values were associated with an interelectrode potential

difference (ΔV) of approximately 4 V and a FE of ~ 41%, due to the predominance of the hydrogen evolution reaction (HER). The final pH was around 7.9, consistent with the buffering action of the bicarbonate system (Eq. (5)-(6)).

$$CO_2 + H_2O \rightleftharpoons H_2CO_3 \rightleftharpoons H^+ + HCO_3^- \quad (5)$$

$$HCO_3^- \rightleftharpoons H^+ + CO_3^{2-} \quad (6)$$

An increase in CO_2 pressure from 1 to 7 bar significantly improved the figures of merit of the process (Fig. 3). As shown in Fig. 3A, the final [FA] increased from 0.25 to 0.32, 0.41, and 0.43 M as P_{CO_2} was raised from 1 to 3, 5, and 7 bar, respectively. This enhancement was primarily driven by a substantial increase in the FE, which rose from 40% to 51%, 65%, and 67%, respectively (Fig. 3B). Consequently, the r_{FA} increased from 1.6 to 2.6 g h^{-1} as P_{CO_2} was elevated from 1 to 7 bar (Fig. 3C). According to the literature, the beneficial effect of increasing P_{CO_2} on CO_2RR is attributed to the higher solubility of CO_2 under pressure, which enhances the rate of mass transport to the cathode surface and promotes its subsequent adsorption (Proietto et al., 2021). The relationship between EC and P_{CO_2} is reported in Fig. 3D. A marked decrease in EC was observed as P_{CO_2} increased from 1 to 7 bar, resulting from both the improvement in FE and a slight reduction in the ΔV, which decreased from approximately 4.0 V at 1 bar to 3.75 V at 7 bar. Further increases in P_{CO_2} to 9, 15, and 20 bar led to lower [FA] values (Fig. 3A) and reduced r_{FA} (Fig. 3C), corresponding to a decrease in FE. For instance, FE declined from 67% at 7 bar to 50% at 20 bar. Accordingly, the plots of FE versus P_{CO_2} (Fig. 3B) and EC versus P_{CO_2} (Fig. 3D) exhibited a maximum and a minimum, respectively. Similar trends have been previously reported for CO_2RR on Ag and Sn electrodes (Proietto et al., 2024; Proietto et al., 2025). To try to understand this trend various factors can be considered:

(i) the increase of the CO_2 pressure gives rise to a decrease of the pH due to the acidic character of H_2CO_3 thus potentially favouring the H_2 evolution which is promoted by a higher H^+ concentration; however, the buffering action of $NaHCO_3$ resulted in a small modification of pH which was in all cases in the range 6.9–7.9;

(ii) it was previously considered that an excessive CO_2 coverage at high pressures is expected to limit the availability of water, protons, and adsorbed hydrogen required for FA formation (Eqs. (7)–(8))

$$CO_2 + H_2O + e^- + * = HCOOad + OH^- \quad (7)$$

$$HCOOad + H_2O + e^- \rightarrow HCOOH + OH^- + * \quad (8)$$

Overall, it is worth noting that operating at a relatively low P_{CO_2} of 7 bar, which entails low operational and capital costs (Proietto et al., 2024), enabled the achievement of an appreciable FE and a quite high final [FA] of 0.47 M. To the best of our knowledge, the highest [FA] values previously reported for $PrCO_2RR$ were approximately 0.3 M.

3.2. *Effect of current intensity*

From an industrial perspective, operating at relatively high I is essential to enhance cell productivity. However, most of the $PrCO_2RR$

Table 1
Effect of [SE] on $PrCO_2RR$*.

[SE]	[FA] (M)	FE (%)	ΔV (V)	EC (kWh mol^{-1})
0.1	0.19	30	4.2	0.70
0.2	0.21	33	4.0	0.65
0.5	0.42	67	3.5	0.31
0.8	0.41	65	3.4	0.28

* $PrCO_2RR$ at Sn cathode and Ti/IrO_2-Ta_2O_5 anode using a water solution (0.4 L) of $NaHCO_3$ under amperostatic conditions (I = 4.5 A) for 3 h with initial P_{CO_2} of 7 bar.

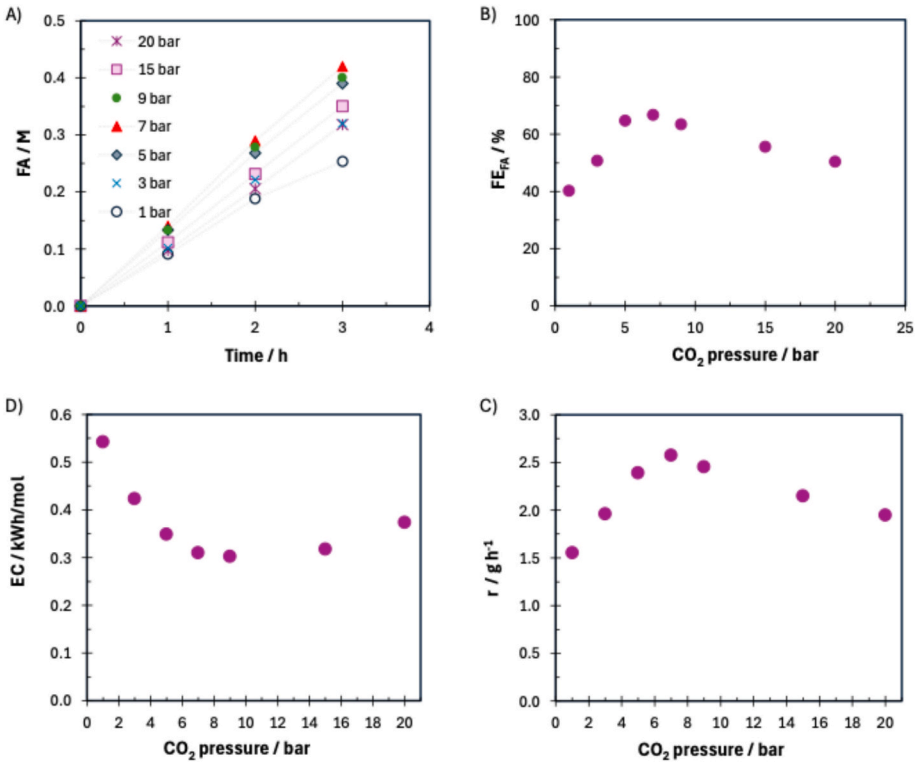

Fig. 3. Effect of P_{CO_2} on $PrCO_2RR$ performed for 3 h in an undivided cell equipped with Sn cathode and Ti/IrO_2-Ta_2O_5 anode using a water solution of 0.5 M $NaHCO_3$ under amperostatic conditions with I = 4.5 A and initial P_{CO_2} of 1, 5, 7, 9, 15 and 20 bar. (A) Plot of [FA] vs time at different P_{CO_2}. Plot of (B) FE_{FA}, (C) EC and (D) r vs P_{CO_2}.

experiments reported in the literature have been conducted at *Is* below 1 A (Table 2). In this work, the effect of *I* and *j* was systematically investigated by performing a series of electrolyses at 7 bar with *Is* of 4.5, 5.6, 8, and 13 A, corresponding to *js* of 0.17, 0.21, 0.30, and 0.50 kA m^{-2}, respectively. As shown in Fig. 4A, increasing *I* from 4.5 to 5.6 A (i.e., from 0.17 to 0.21 kA m^{-2}) led to a rise in the final [FA] from 0.42 to 0.47 M after 3 h, attributable to the higher total charge passed (+24%), which was only partially offset by a moderate decrease in FE from 68% to 61%. Consequently, the cell productivity increased from 2.6 to 2.9 g h^{-1} (Fig. 4C), while the corresponding EC showed a slight increase (Fig. 4D). However, further increasing *I* beyond 5.6 A (0.21 kA m^{-2}) resulted in lower [FA] values (Fig. 4A), reduced r_{FA} (Fig. 4C), and higher EC (Fig. 4D). This decline in performance was primarily due to a pronounced decrease in FE, which counteracted the benefit of the larger charge passed.

To rationalize the detrimental effect observed at high *I*, it is important to note that elevated *I* and *j* are expected to decrease CO_2 surface coverage, thereby promoting the competitive adsorption of hydrogen species and enhancing the hydrogen evolution reaction (HER) (Proietto et al., 2024). Consequently, the negative influence of high *I* on FE may be mitigated or even prevented by operating at higher P_{CO_2}. Therefore, the effect of *I* was also investigated at 20 bar. As shown in Fig. 4A and 5A, increasing P_{CO_2} substantially improved the process performance. Under these conditions, increasing *I* up to 13 A (0.5 kA m^{-2}) led to a marked enhancement in FA production. Specifically, raising *I* from 4.5 to 8 and 13 A (i.e., from 0.17 to 0.3 and 0.5 kA m^{-2}) resulted in final [FA] values of 0.3, 0.6, and 0.8 M, respectively (Fig. 5A), with corresponding r_{FA} of approximately 2.0, 4.0, and 5.2 g h^{-1} (Fig. 5B). These improvements were associated with the larger total charge passed and FE values exceeding 50% (Fig. 5B). However, further increasing *I* to 20 A (0.75 kA m^{-2}) led to a sharp decline in r_{FA} (Fig. 5A and C) and a significant rise in EC (Fig. 5D), as a consequence of the pronounced drop in FE (Fig. 5B). Overall, these results indicate that increasing P_{CO_2} effectively enables operation at higher *I* with satisfactory performance, although excessively high *I* remains detrimental to process efficiency.

3.3. Coupled effect of I and P_{CO_2}

As shown in the previous section, the effect of *I* strongly depends on the adopted P_{CO_2} and vice versa. Hence, to evaluate the coupled effect of *I* and P_{CO_2}, a large series of electrolyses was carried out changing both *I* and P_{CO_2}. Fig. 6 reports the results achieved after 3 h by changing P_{CO_2} at various values of *I*. It is clearly shown that:

- the optimal value of P_{CO_2} in terms of r_{FA} strongly depends on the adopted *I* and it increased with *I* (Fig. 6A and 6B), thus confirming that a proper balance between P_{CO_2} and *I* is necessary; as an example, the optimal values of P_{CO_2} were 7 bar at 4.5 A (r_{FA} = 2.6 g h^{-1}) and 20 bar at 13 A., corresponding to 0.5 kA m^{-2} (r_{FA} = 5.2 g h^{-1});
- similarly, the optimal value of *I* in terms of r_{FA} strongly depends on adopted P_{CO_2} and it increased with P_{CO_2}: as an example, the optimal values of *I* were 4.5 (0.17 kA m^{-2}) and 13A (0.3 kA m^{-2}) for P_{CO_2} of 7 and 20 bar, respectively (Fig. 6D and 6E);
- the highest values of both [FA] (0.85 M) and r_{FA} (5.2 g h^{-1}) were achieved coupling intermediate values of both *I* (13 A) and P_{CO_2} (20 bar);
- too high values of both P_{CO_2} and *I* were not useful to increase the r_{FA} (Fig. 6B and E).

Moreover, it was shown that the EC in most of cases decreased with P_{CO_2} because of both the increase of the r_{FA} and the decrease of the ΔV even if too high P_{CO_2} resulted in an increase of EC (Fig. 6C). As an example, at 13 A the increase of P_{CO_2} from 1 to 20 bar resulted in a decrease of EC from 3.05 to 0.47 kWh mol^{-1} (Fig. 6C) because of the increase of [FA] from 0.16 to 0.85 M (Fig. 6A) coupled with the decrease of ΔV from 5 to 4.7 V. However, a further increase of P_{CO_2} to 30 bar gave rise to a slight increase of EC (0.5 kWh mol^{-1}) due to the slight decrease of r_{FA} (Fig. 6A and B). Conversely, the increase of *I* resulted usually in an increase of EC (Fig. 6F) due mainly to the enhancement of the charge passed for the same amount of time and of ΔV; as an example, at 15 bar, EC increased from 0.30 to 0.39 and 0.69 kWh mol^{-1} upon increasing *I* from 4.5 to 8 and 13 A (i.e., from 0.17 to 0.3 and 0.5 kA m^{-2}) because the increase of [FA] (from 0.36 to 0.6 and 0.74 M) was partially wasted by the higher amount of charge passed and by a significant increase of

Table 2
Comparison with some electrochemical performances for $PrCO_2CR$ into FA reported in literature.

Entry	P_{CO_2} (bar)	*j* (mA cm^{-2})	*I* (A)	Area (cm^2)	Type of cell	Cathode	Electrolyte	Time	[FA] (mM)	FE (%)	Ref.
1	23	−50	0.45	9	Undivided	Sn foil	0.1 M Na_2SO_4	43 h	273	82	(Proietto et al., 2018)
2	30	−163	0.026	0.16	Divided	Sn wire	0.1 M $KHCO_3$	3.2 h	NA	92	(Hara et al., 1995)
3	50	−30	2.4	80	Divided	Sn plate	0.25 M K_2SO_4	20 min	217	90	(Ramdin et al., 2019)
4	30	−593	0.59	1[a]	Divided	Bi nanosheets	2 M $KHCO_3$	30 min	82[b]	90	(Ruan et al., 2022)
5	56	−500	0.035	0.07	Undivided	POD-Bi	0.5 M $KHCO_3$	~ 27 min	0.26mmol[c]	91	(He et al., 2018)
6	10	−75	0.113	1.5	Undivided	Bi rod	0.1 M Na_2SO_4	30 h	80	92	(Proietto et al., 2023)
7	40	−150	0.36	2.4	Undivided	Sn foil	0.5 M $KHCO_3$	2 h	235	90	(Proietto et al., 2025)
8	56	−190	0.45	2.4	Undivided	Bi foil	0.5 M $KHCO_3$	2 h	268	80	(Proietto et al., 2025)
9	55	−50	0.12	2.4	Undivided	Ni foil	0.5 M $KHCO_3$	2 h	30	36	(Proietto et al., 2025)
10	100	−2	0.002	1	Divided	Cu based catalyst	0.1 M $KHCO_3$	12 h	NA	20	(Qiu et al., 2023)
11	40	−3542	1.7	0.5	Divided	2D Bi_2O_2Se electrode	0.5 M $KHCO_3$	NA	NA	78	(Sun et al., 2025)
12	7 or 20	21–50	5.6 or-13	260	Undivided	Sn foil	0.5 M $NaHCO_3$	3–8 h	800—1100	66—51	This work

NA: not available in the related paper.
[a] ECSA = 58 cm^2.
[b] Estimated by these authors considering the information of the related reference: V = 60 mL and 9.9 mmol h^{-1} cm^{-2}.
[c] Estimated by these authors considering the information of the related reference: r = 391 mg h^{-1} cm^{-2} MW: 46 g mol^{-1}.

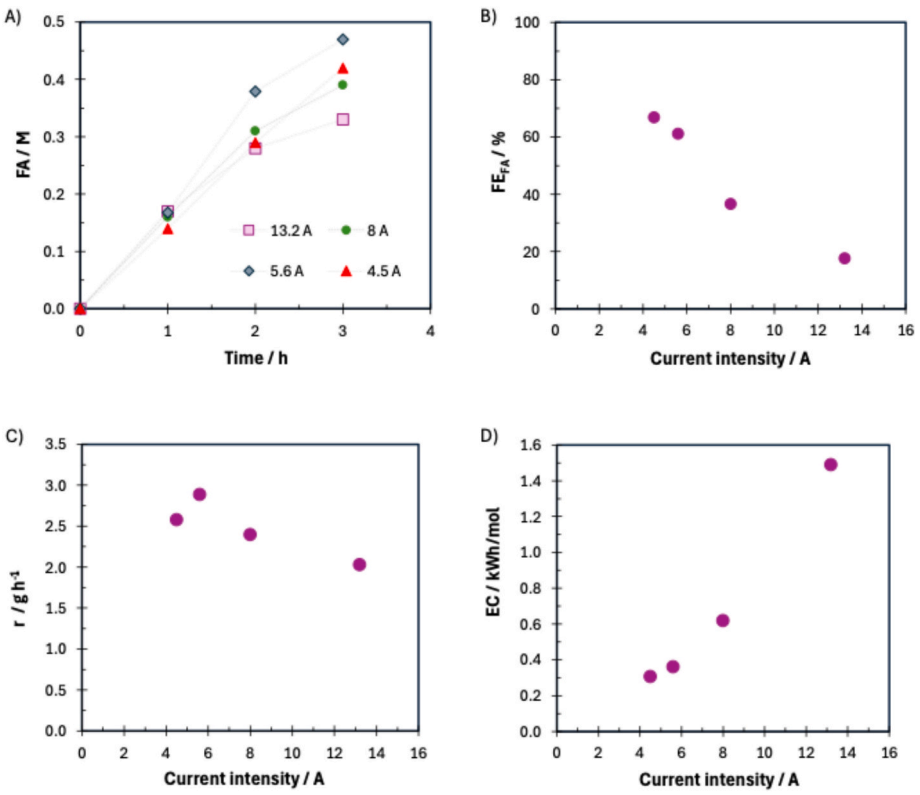

Fig. 4. Effect of *I* on $PrCO_2RR$ performed for 3 h in an undivided cell equipped with Sn cathode and Ti/IrO_2-Ta_2O_5 anode using a water solution of 0.5 M $NaHCO_3$ under amperostatic conditions with P_{CO_2} = 7 bar. (A) Plot of [FA] vs time at different *I*. Plot of (B) FE_{FA}, (C) r and (D) EC vs *I*.

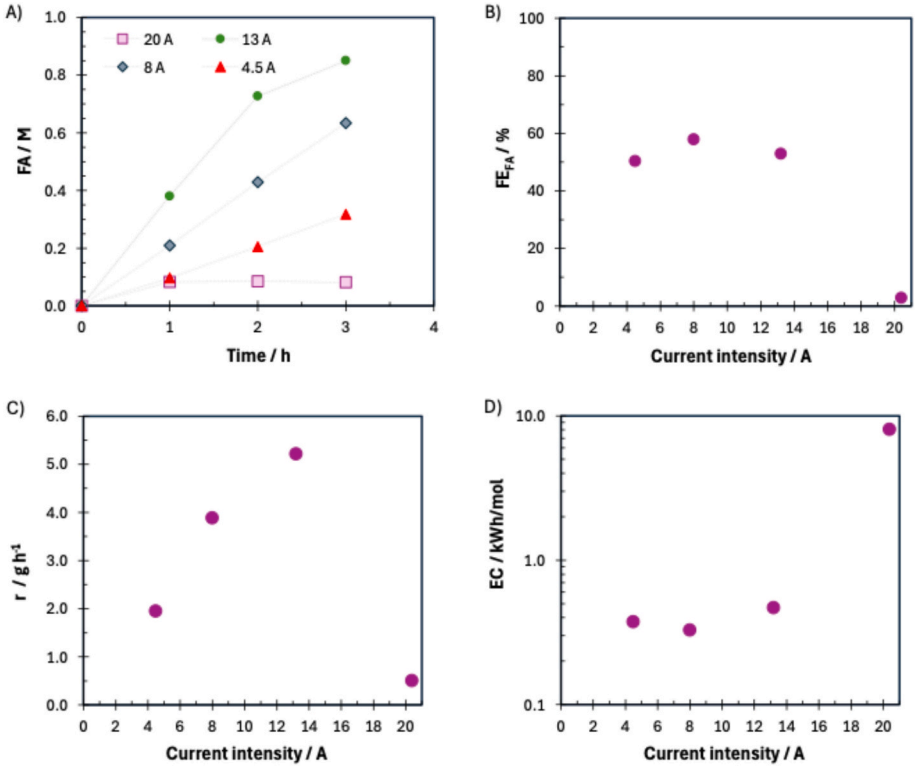

Fig. 5. Effect of *I* on $PrCO_2RR$ performed for 3 h in an undivided cell equipped with Sn cathode and Ti/IrO_2-Ta_2O_5 anode using a water solution of 0.5 M $NaHCO_3$ under amperostatic conditions with $\boldsymbol{P_{CO_2}}$ = 20 bar. (A) Plot of [FA] vs time at different *I*. Plot of (B) FE_{FA}, (C) r and (D) EC vs *I*.

ΔV (from 3.3 to 4.0 and 4.6 V).

High values of *I* and *j* are expected to affect negatively the production of FA due to various complementing effects: (i) gas bubble accumulation (Martens et al., 2023), (ii) temperature increase (Proietto et al., 2023),

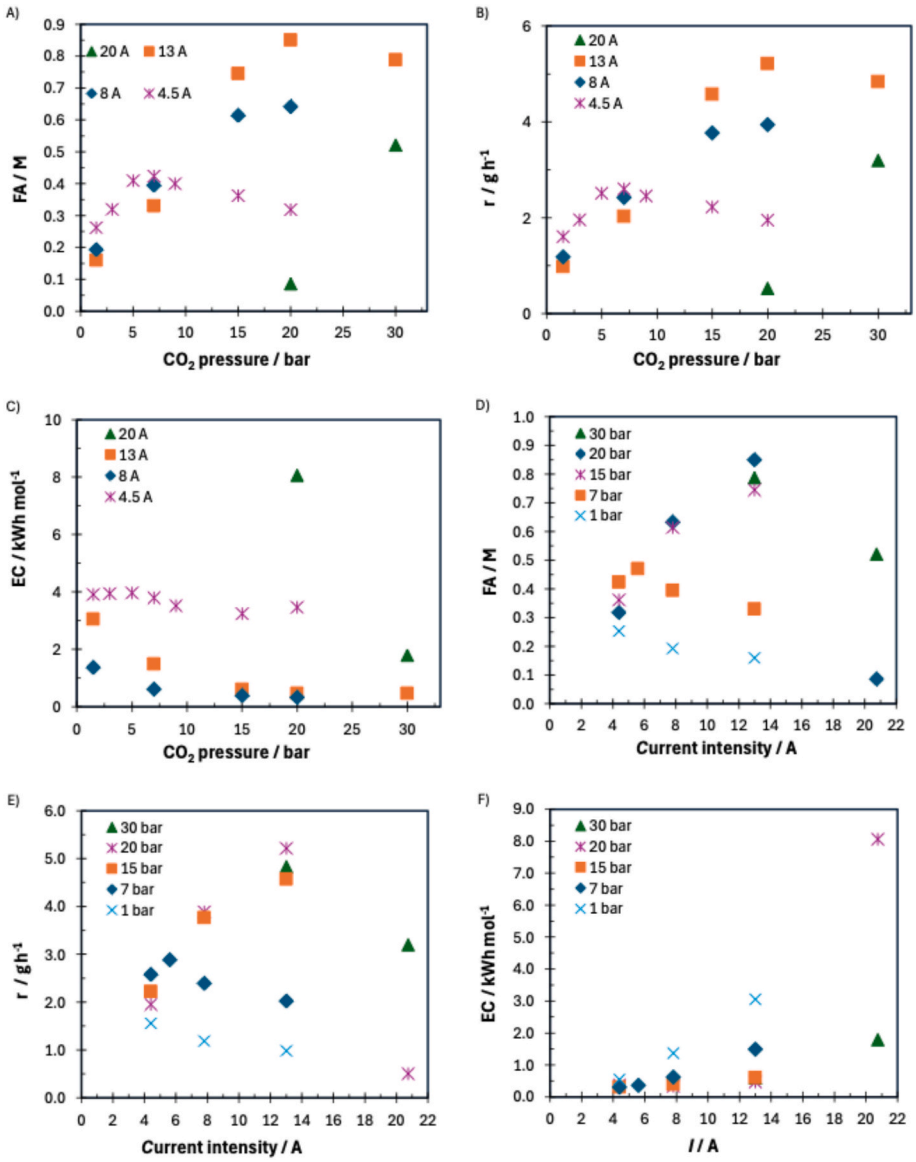

Fig. 6. Coupled effect of I and P_{CO_2} on $PrCO_2RR$ at Sn cathode and Ti/IrO_2-Ta_2O_5 anode using a water solution of 0.5 M $NaHCO_3$ under amperostatic conditions for 3 h. Plot of (A) [FA], (B) FE_{FA} and (C) EC vs. P_{CO_2} at different I. Plot of (D) [FA], (E) FE_{FA} and (F) EC vs. I at different P_{CO_2}.

(iii) high pH gradient between the cathode surface and (iv) lower coverage of the surface by CO_2. In particular, the use of high I is expected to cause a small increase of the temperature in the diffusion layer, and it was previously shown that the $PrCO_2RR$ is significantly favored by low temperatures (Proietto et al., 2023). Moreover, we have verified by experiments performed in conventional lab glass cells that at these js part of the electrode is covered by gas bubbles that reduce the active surface. Higher I may also create mass transfer limitations, that were prevented in our case by the high concentrations of CO_2 present in the bulk due to the use of relatively high CO_2 pressures; indeed, the limiting js for a process under the kinetic control of the mass transfer of CO_2 to the cathode surface were significantly higher than adopted js.

To better understand the coupled effect of I and P_{CO_2}, it is useful to consider the reaction mechanism for the $PrCO_2RR$ to FA at tin cathodes. The process can be described by the adsorption of CO_2 (eq. (9)), the cathodic reduction of adsorbed CO_2 (eq. (10)) and following reduction to HCOOH and desorption (Eqs. (11) and (12)).

$$CO_{2(aq.)} + * = CO2_{(ad)} \quad (9)$$

$$CO_{2(ad)} + H^+ + e^- = OCOH_{(ad)} \quad (10)$$

$$OCOH_{(ad)} + H^+ + e^- = HCOOH_{(ad)} \quad (11)$$

$$*HCOOH \rightarrow * + HCOOH \quad (12)$$

According to Proietto et al. (Proietto et al., 2019), the rate determining step of $PrCO_2RR$ to FA at tin cathodes involves the reduction of adsorbed CO_2 and it can be described by a Langmuir-Hinshelwood type expression ($r = k(E)\, b\, [CO_2]/(1 + b\, [CO_2])$; hence, for a fixed value of I, r is expected to increase proportionally to $[CO_2]$ (and to P_{CO_2}) for lower values of P_{CO_2} and to tend to a plateau value for high values of P_{CO_2}. This model well illustrates why the production of FA increases with P_{CO_2} up to a maximum value but does not explain the decreased values of [FA] observed for rather high values of P_{CO_2}. To explain this trend, it was recently proposed that a very high coverage of CO_2 limits the presence of protons and water necessary to produce FA (Proietto et al., 2024). To understand the negative effect of high I on the production of FA, it is useful to highlight that high currents are expected to reduce the coverage of the surface by CO_2, thus favouring the competitive adsorption of H and the hydrogen evolution (Proietto et al., 2024), if they are not sufficiently compensated by high concentrations of CO_2

imposed by adequate P_{CO_2}.

3.4. Effect of concentration of SE and time

Some authors have reported that the performance of CO_2RR can depend on the concentration of the supporting electrolyte (SE). In the previous section, it was highlighted that an increase in *I* is often associated with an increase of ΔV, leading to a higher EC. This effect could potentially be mitigated by using more concentrated SE solutions. To investigate this aspect, the influence of [SE] was studied by performing a series of electrolyses at 7 bar and 4.5 A for 3 h using $NaHCO_3$ solutions with different concentrations: 0.1, 0.2, 0.5, and 0.8 M.

According to the literature, the [SE] concentration can affect the process in various ways:

- High [SE]s reduce the CO_2 solubility. For example, according to the literature, at CO_2 pressures close to 8 bar for T = 313 K, the increase of [$NaHCO_3$] from 0.1 to 0.8 M gives rise to a decrease of the CO_2 solubility in water of about 20% (Han et al., 2011).
- The [SE] increase was reported to favour the hydrogen evolution with respect to CO_2 evolution for experiments performed with a P_{CO2} of 1 bar with low *j*s (Proietto et al., 2024).
- Higher electrolyte concentrations enhance the ionic conductivity of the solution, thereby reducing ohmic losses and mitigating both cell potential and local temperature peaks during electrolysis.
- An increase in $NaHCO_3$ concentration promotes a higher local CO_2 availability through the equilibria described in Eqs. ((5)-(6)).

Hence, the overall effect of [SE] is expected to depend stronlgly on adopted operative conditions.

As shown in Table 1, [SE] had a strong and positive impact on process performance. The final [FA] was approximately 0.2 M for the lowest [SE] value and increased to about 0.4 M for [SE] of 0.5 and 0.8 M. In addition, increasing [SE] reduced the cell potential from 4.2 V at 0.1 M to 3.4 V at 0.8 M. Consequently, when using 0.8 M $NaHCO_3$, the EC decreased to approximately 0.28 kWh mol^{-1}, which is significantly lower than the 0.70 kWh mol^{-1} observed at 0.1 M SE.

The final [FA] value is highly relevant from an economic perspective. Indeed, higher [FA] directly reduce the costs associated with downstream concentration steps required to obtain aqueous formate solutions at marketable concentrations. As reported in Table 2, the [FA] values achieved in this study are the highest reported so far for PrCO_2RR. To further enhance the final [FA], additional electrolysis experiments were carried out for 8 h at 7 bar, applying currents of 4.5 and 5.6 A (conditions that had yielded the best results in 3 h trials at the same pressure). High [SE] values (0.8 and 1.0 M) were employed to minimizeEC.

Electrolyses performed at 4.5 A (Fig. 7A) resulted in a stable FA production, with a nearly constant FE slightly above 60%, up to 6 h (Fig. 7B). After 6 h, [FA] reached 0.77 M, subsequently increasing to 0.86 M after 8 h, although the FE decreased to 51%. According to recent literature, experiments performed using carbon-free bismuth (Bi) and tin (Sn)- based GDEs, in divided cells gave quite stable FE for almost 200 h at 100 mA cm^{-2} (Singh et al., 2026). The authors found that performance degradation took place after 200 h and that it was predominantly influenced by changes in electrolyte properties, specifically pH and conductivity, rather than intrinsic catalyst failure. The slight FE decrease observed after 8 h in this work is probably related to the fact that the electrolyses were performed in undivided cells, thus potentially allowing the anodic oxidation of formate to CO_2, which can lower the overall FE. Furthermore, this anodic oxidation process is expected to be promoted at high FA concentrations. (Proietto et al., 2021). To evaluate the impact of the anodic process, a series of electrolyses was performed in the absence of CO_2 with an initial concentration of FA of 0.1, 0.2 or 0.3 M. It was shown that the oxidation of FA at the adopted cathode (Ti/IrO_2–Ta_2O_5) is negligible when an initial [FA] of 0.1 M is used, but it takes place in a significant way even if with a FE lower than 20% when the initial [FA] is increased to 0.2 or 0.3 M, thus confirming the negative impact of this anodic process on the electrochemical reduction of CO_2 at high [FA]. The results obtained at 4.5 A and 7 bar demonstrate that it is indeed possible to achieve high [FA] values in undivided cells while maintaining a relatively high FE, due to the fact that the cathodic reduction of CO_2 to FA at Sn cathodes takes place with very high selectivity with respect to the anodic oxidation of FA at Ti/IrO_2–Ta_2O_5 anodes. However, it will be necessary in the future to devote a focused study aimed to minimize the anodic oxidation of FA.

When the current was increased to 5.6 A, previously identified as optimal for 3 h experiments at 7 bar (Fig. 4A), the [FA] rose almost linearly during the first 6 h, with FE values between 65 and 67% (Fig. 7B), reaching 1.0 M. Beyond 6 h, [FA] continued to increase up to 1.1 M, though with progressively decreasing FE values.

It is worth noting that, to the best of our knowledge, the [FA] values obtained in this work are the highest reported to date for PrCO_2RR performed in undivided cells and among the highest achieved in divided ones. Table 2 summarizes several results reported in the literature for pressurized CO_2 reduction to FA using different cathode materials in both divided and undivided cell configurations. The highest [FA] values previously reported were approximately 0.3 M (entries 1, 7, and 8), obtained with Sn and Bi cathodes. In contrast, the present study achieved [FA] values up to 1.1 M with simple Sn plate cathode. High [FA] concentrations have also been reported for non-pressurized systems employing gas diffusion electrodes (GDEs) in divided cells, although these typically remain below 0.5 M. (Proietto et al., 2021) A notable exception is the work of Yang et al. (Yang et al., 2017), who achieved a final [FA] close to 2.0 M using a rather complex three-compartment cell design, consisting of an anode compartment, an intermediate flow chamber containing a cation-exchange resin (Amberlite), and a cathode compartment where electrochemical CO_2 reduction to formate occurs on a Sn-based GDE. In contrast, the PrCO_2RR system developed in this

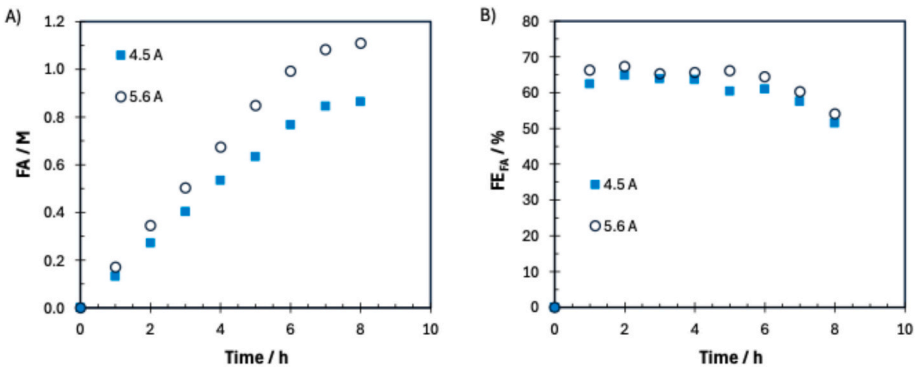

Fig. 7. Effect of time on (A) [FA] and (B) FE_{FA} during PrCO_2RR using Sn cathode and Ti/IrO_2-Ta_2O_5 anode using a water solution of 0.5 M $NaHCO_3$ under amperostatic conditions (4.5 and 5.6 A) with P_{CO_2} = 7 bar.

study employs a simple, low-cost undivided cell configuration equipped with low-cost electrodes, significantly enhancing the economic attractiveness and scalability of the proposed method.

4. Conclusion

This study systematically investigated the pressurized electrochemical reduction of CO_2 to FA ($PrCO_2RR$) using a tin plate cathode in a simple undivided cell configuration, operating at I between 4 and 20 A. The effects of key parameters, including I, P_{CO_2} (1–30 bar), supporting electrolyte concentration, and electrolysis duration, were evaluated to optimize performance in terms of final [FA], r_{FA}, and EC. The best results were achieved under intermediate values of both I and P_{CO_2}, which enabled high productivity and [FA] values in the range of 0.7–1.1 M, surpassing significantly previously reported data for $PrCO_2RR$. The main findings can be summarized as follows:

- both [FA] vs. P_{CO_2} and [FA] vs. I plots exhibited a clear maximum;
- the optimal P_{CO_2} increased with I, confirming the need for a proper balance between these parameters; for instance, optimal P_{CO_2} values were 7 bar at 4.5 A and 20 bar at 13 A;
- similarly, the optimal I increased with P_{CO_2}: at 7 and 20 bar, the best performances were observed at 4.5 and 13 A, respectively;
- higher supporting electrolyte concentrations (0.5–0.8 M $NaHCO_3$) reduced ΔV and EC, while longer electrolysis times (up to 8 h) further enhanced [FA].

Overall, these results demonstrate that the combination of moderate P_{CO_2}, optimized I, and adequately concentrated electrolytes enables highly efficient, low-cost, and scalable electrochemical production of FA. However, further investigations will be necessary to enhance the scalability of this apparatus for large-scale applications. In particular, this process, especially if performed in undivided cells, may be affected by the potential formation of an explosive H_2/O_2 mixture. Therefore, future research will focus on this issue, and several strategies will be explored, including: (i) the implementation of sacrificial anodes to suppress the oxygen evolution reaction; (ii) the development of pressurized coupled processes that replace oxygen evolution with the production of compounds characterized by higher economic value and improved safety profiles; (iii) the use of more selective cathodes (e.g., mesh electrodes) to suppress or minimize hydrogen production at high pressure; and (iv) the development of a novel reactor configuration operating in continuous mode, aimed at preventing the mixing of the potentially formed cathodic co-product (hydrogen) with the anodic product (oxygen), while also increasing the conversion rate.

CRediT authorship contribution statement

Pengfei Ma: Writing – original draft, Supervision, Project administration, Methodology, Funding acquisition, Data curation, Conceptualization. **Xinya Wang:** Methodology, Investigation, Data curation. **Federica Proietto:** Writing – review & editing, Validation, Methodology, Data curation, Conceptualization. **Xianming Zhang:** Writing – review & editing, Validation, Supervision, Resources, Conceptualization. **Onofrio Scialdone:** Writing – original draft, Supervision, Conceptualization.

Declaration of competing interest

The authors declare that they have no known competing financial interests or personal relationships that could have appeared to influence the work reported in this paper.

Acknowledgments

This work was supported by MUR (PRIN 2022, Electrochemical conversion of carbon dioxide: towards sustainable electrochemical production of formic acid) and the Tangshan Sanyou Group Co., Ltd.

Data availability

Data will be made available on request.

References

Bushuyev, O.S., De Luna, P., Dinh, C.T., Tao, L., Saur, G., Van De Lagemaat, J., Kelley, S. O., Sargent, E.H., 2018. What should we make with CO_2 and how can we make it? Joule 2, 825–832. https://doi.org/10.1016/j.joule.2017.09.003.

Chen, B., Feng, M., Chen, Y., Jirui, Y., Liu, Y., 2024. Performing electrocatalytic CO_2 reduction reactions at a high pressure. Carbon Neutrality 3, 31. https://doi.org/10.1007/s43979-024-00106-7.

Dufek, E.J., Lister, T.E., Stone, S.G., McIlwain, M.E., 2012. Operation of a pressurized system for continuous reduction of CO_2. J. Electrochem. Soc. 159, F514–F517. https://doi.org/10.1149/2.011209jes.

Gabardo, C.M., Seifitokaldani, A., Edwards, J.P., Dinh, C.-T., Burdyny, T., Kibria, M.G., O'Brien, C.P., Sargent, E.H., Sinton, D., 2018. Combined high alkalinity and pressurization enable efficient CO_2 electroreduction to CO. Energy Environ. Sci. 11, 2531–2539. https://doi.org/10.1039/c8ee01684d.

Girichandran, N., Saedy, S., Kortlever, R., 2024. Electrochemical CO_2 reduction on a copper foam electrode at elevated pressures. Chem. Eng. J. 487, 150478. https://doi.org/10.1016/j.cej.2024.150478.

Han, X., Yu, Z., Qu, J., Qi, T., Guo, W., Zhang, G., 2011. Measurement and correlation of solubility data for CO_2 in NaHCO3 aqueous solution. J. Chem. Eng. Data 56, 1213–1219. https://doi.org/10.1021/je1011168.

Hara, K., Tsuneto, A., Kudo, A., Sakata, T., 1994. Electrochemical reduction of CO_2 on a Cu electrode under high-pressure - factors that determine the product selectivity. J. Electrochem. Soc. 141, 2097–2103. https://doi.org/10.1149/1.2055067.

Hara, K., Kudo, A., Sakata, T., 1995. Electrochemical reduction of carbon dioxide under high pressure on various electrodes in an aqueous electrolyte. J. Electrochem. Soc. 391, 141–147. https://doi.org/10.1016/0022-0728(95)03935-A.

He, S., Ni, F., Ji, Y., Wang, L., Wen, Y., Bai, H., Liu, G., Zhang, Y., Li, Y., Zhang, B., Peng, H., 2018. The p-orbital delocalization of main-group metals to boost CO_2 electroreduction. Angew. Chem. Int. Ed. 57, 16114–16119. https://doi.org/10.1002/anie.201810538.

Heuser, S., Hoof, L., Pellumbi, K., Oberndorf, J.N., Krämer, L., Blaudszun, D., Puring, K.j., Prokein, M., Mölders, N., Kilzer, A., Petermann, M., Apfel, U.-P., 2025. Differential pressure CO_2 electrolysis opens the way for direct coupling to industrial processes. Chem Catal. 5 (8). https://doi.org/10.1016/j.checat.2025.101393.

Huang, L., Gao, G., Yang, C., Li, X.-Y., Miao, R.K., Xue, Y., Xie, K., Ou, P., Yavuz, C.T., Han, Y., Magnotti, G., Sinton, D., Sargent, E.H., Lu, W., 2013. Pressure dependence in aqueous-based electrochemical CO_2 reduction Nat. Commun 14, 2958. https://doi.org/10.1038/s41467-023-38775-0.

Huang, Z., Grim, R.G., Schaidle, J.A., Tao, L., 2021. The economic outlook for converting CO_2 and electrons to molecules. Energy Environ. Sci. 14, 3664–3678. https://doi.org/10.1039/d0ee03525d.

Muhammad Shakir Hussain, Sheraz Ahmed, Chirong Sun, Hyung-Suk Oh, Jaehoon Kim. Boosting electrochemical CO_2 reduction to CO by regulating pressure in zero-gap electrolyzer. Journal of CO_2 Utilization 100 (2025) 103179. 10.1016/j.jcou.2025.103179.

Izadi, P., Varhade, S., Carl, S., Haus, P., Singh, C., Guruji, A., Pant, D., Harnisc, F., 2026. Scaling up electrochemical CO2 reduction to formate through comparative reactor analysis. Ind. Chem. Mater. https://doi.org/10.1039/D5IM00056D.

Köleli, F., Balun, D., 2004. Reduction of CO_2 under high pressure and high temperature on Pb-granule electrodes in a fixed-bed reactor in aqueous medium. Appl. Cataly. A-Gen. 274, 237–242. https://doi.org/10.1016/j.apcata.2004.07.006.

Kudo, A., Nakagawa, S., Tsuneto, A., Sakata, T., 1993. Electrochemical reduction of high-pressure CO_2 on Ni electrodes. J. Electrochem. Soc. 140, 1541–1545. https://doi.org/10.1149/1.2221599.

Lamaison, S., Wakerley, D., Blanchard, J., Montero, D., Rousse, G., Mercier, D., Marcus, P., Taverna, D., Giaume, D., Mougel, V., Fontecave, M., 2020. High-current-density CO_2-to-CO electroreduction on Ag-alloyed Zn dendrites at elevated pressure. Joule 4, 395–406. https://doi.org/10.1016/j.joule.2019.11.014.

Leonzio, G., Hankin, A., Shah, N., 2024. CO_2 electrochemical reduction: a state-of-the-art review with economic and environmental analyses. Chem. Eng. Res. Des. 208, 934–955. https://doi.org/10.1016/j.cherd.2024.07.014.

Li, J., Kuang, Y., Meng, Y., Tian, X., Hung, W.-H., Zhang, X., Li, A., Xu, M., Zhou, W., Ku, C.-S., Chiang, C.-Y., Zhu, G., Guo, J., Sun, X., Dai, H., 2020. Electroreduction of CO_2 to formate on a copper-based electrocatalyst at high pressures with high energy conversion efficiency. J. Am. Chem. Soc. 142, 7276–7282. https://doi.org/10.1021/jacs.0c00122.

Martens, C., Schmid, B., Tempel, H., Eichela, R.-A., 2023. CO_2 flow electrolysis – limiting impact of heat and gas evolution in the electrolyte gap on current density. Green Chem. 25, 7794.

Masel, R.I., Liu, Z., Yang, H., Kaczur, J.J., Carrillo, D., Ren, S., Salvatore, D., Berlinguette, C.P., 2021. An industrial perspective on catalysts for low-temperature CO_2 electrolysis. Nat. Nanotechnol. 16, 118–128. https://doi.org/10.1038/s41565-020-00823-x.

Mizuno, T., Ohta, K., Sasaki, A., Akai, T., Hirano, M., Kawabe, A., 1995. Effect of temperature on electrochemical reduction of high-pressure CO2 with In, Sn, and Pb

electrodes. Energy Sources 17, 503–508. https://doi.org/10.1080/00908319508946098.
Morrison, A.R.T., van Beusekom, V., Ramdin, M., van den Broeke, L.J.P., Vlugt;, T.J.H., de Jong, W., 2019. Modeling the electrochemical conversion of carbon dioxide to formic acid or formate at elevated pressures. J. Electrochem. Soc. 166, E77–E86. https://doi.org/10.1149/2.0121904jes.
Morrison, A.R.T., Girichandran, N., Wols, Q., Kortlever, R., 2023. Design of an elevated pressure electrochemical flow cell for CO_2 reduction. J. Appl. Electrochem. 53, 2321–2330. https://doi.org/10.1007/s10800-023-01927-7.
Philips, M.F., Gutter, G.J.M., Koper, M.T.M., Schouten, K.J.P., 2020. Optimizing the electrochemical reduction of CO_2 to formate: a state-of-the-art analysis. ACS Sustain. Chem. Eng. 8, 15430–15444. https://doi.org/10.1021/acssuschemeng.0c05215.
Proietto, F., Schiavo, B., Galia, A., Scialdone, O., 2018. Electrochemical conversion of CO_2 to HCOOH at tin cathode in a pressurized undivided filter-press cell. Electrochim. Acta 277, 30–40. https://doi.org/10.1016/j.electacta.2018.04.159.
Proietto, F., Galia, A., Scialdone, O., 2019. Electrochemical conversion of CO_2 to HCOOH at tin cathode: development of a theoretical model and comparison with experimental results. ChemElectroChem 6, 162–172. https://doi.org/10.1002/celc.201801067.
Proietto, F., Patel, U., Galia, A., Scialdone, O., 2021. Electrochemical conversion of CO_2 to formic acid using a Sn based electrode: a critical review on the state-of-the-art technologies and their potential. Electrochim. Acta 389, 138753. https://doi.org/10.1016/j.electacta.2021.138753.
Proietto, F., Berche, F., Galia, A., Scialdone, O., 2021. Electrochemical conversion of pressurized CO_2 at simple silver-based cathodes in undivided cells: study of the effect of pressure and other operative parameters. J. Appl. Electrochem. 51, 267–282. https://doi.org/10.1007/s10800-020-01505-1.
Proietto, F., Galia, A., Scialdone, O., 2021. Towards the electrochemical conversion of CO_2 to formic acid at an applicative scale: technical and economic analysis of most promising routes. ChemElectroChem 8, 2169–2179. https://doi.org/10.1002/celc.202100213.
Proietto, F., Li, S., Loria, A., Hu, X.-M., Galia, A., Ceccato, M., Daasbjerg, K., Scialdone, O., 2022. High-pressure synthesis of CO and syngas from CO_2 reduction using Ni−N-doped porous carbon electrocatalyst. J. Chem. Eng. 49, 132251. https://doi.org/10.1016/j.cej.2021.132251.
Proietto, F., Rinicella, R., Galia, A., Avila-Bolívar, B., Montiel, V., Solla-Gullón, J., Scialdone, O., 2023. Cathodic reduction of CO_2 to formic acid: effect of the nature of the cathode for pressurized systems. J. Environ. Chem. Eng. 11, 109903. https://doi.org/10.1016/j.jece.2023.109903.
Proietto, F., Rinicella, R., Galia, A., Scialdone, O., 2023. Electrochemical conversion of CO_2 to formic acid using a Sn based cathode: combined effect of temperature and pressure. J. CO2 Util. 67, 102338. https://doi.org/10.1016/j.jcou.2022.102338.
Proietto, F., Cammisa, G., Contino, M., Inguanta, R., Galia, A., Scialdone, O., 2024. Cathodic conversion of pressurized CO_2 at silver cathodes: what are the optimal values of pressure and current density? ChemSusChem 17. https://doi.org/10.1002/cssc.202400440.
Proietto, F., Miceli, C., Meli, P., Galia, A., Scialdone, O., 2024. Conversion of CO_2 to formic acid in a microfluidic electrochemical cell with and without supporting electrolyte. J. Environ. Chem. Eng. 12, 112472.
Proietto, F., Raso, S.L., Prestigiacomo, C., Galia, A., Scialdone, O., 2025. Role of pressure and current density on the cathodic conversion of CO_2 using Ag, Sn, Bi and Ni cathodes. J. Environ. Chem. Eng. 13 (5), 117871. https://doi.org/10.1016/j.jece.2025.117871.
Qiu, R., Jia, J., Peng, L.i., Li, R., Yan, S., Li, J., Zhang, J., Sun, D.T., Lan, Z., Xue, T., Guangkuo, Xu., Cui, L., Lv, Z., Li, C., Hong, Y., Guo, Y., Ren, B., Yang, S., Li, J., Han, B., 2023. Enhanced electroreduction of CO_2 to ethanol via enriched intermediates at high CO_2 pressures. Green Chem. 25, 684. https://doi.org/10.1039/D2GC03343G.
Ramdin, M., Morrison, A.R.T., de Groen, M., van Haperen, R., de Kler, R., van den Broeke, L.J.P., Trusler, J.P.M., de Jong, W., Vlugt;, T.J.H., 2019. High pressure electrochemical reduction of CO_2 to formic acid/formate: a comparison between bipolar membranes and cation exchange membranes. Ind. Eng. Chem. Res. 58, 1834–1847. https://doi.org/10.1021/acs.iecr.8b04944.
Ruan, S., Zhang, B., Zou, J., Zhong, W., He, X., Lu, J., Zhang, Q., Wang, Y., Xie, S., 2022. Bismuth nanosheets with rich grain boundaries for efficient electroreduction of CO_2 to formate under high pressures. Chin. J. Catal. 43 (12), 3161–3169. https://doi.org/10.1016/s1872-2067(22)64131-7.
Scialdone, O., Galia, A., Lo Nero, G., Proietto, F., Sabatino, S., Schiavo, B., 2016. Electrochemical reduction of carbon dioxide to formic acid at a tin cathode in divided and undivided cells: effect of carbon dioxide pressure and other operating parameters. Electrochim. Acta 199, 332–341. https://doi.org/10.1016/j.electacta.2016.02.079.
Singh, C., Song, J., Prasannachandran, R., Grijalvo, A., Shen, J., Chen, Z., Vaes, J., Birdja, Y.Y., Pant, D., 2026. Unlocking long-term stability in metal-based gas diffusion electrodes for CO_2 electroreduction. EES Catal. 4, 97–107.
Sun, R., Zhao, J., Liu, H., Yanrong Xue, X.L., 2025. Pressure regulated CO_2 electrolysis on two-dimensional Bi_2O_2Se Chem. Commun 61, 2071. https://doi.org/10.1039/D4CC05357E.
Tang, C., Gong, P., Xiao, T., Sun, Z., 2021. Direct electrosynthesis of 52% concentrated CO on silver's twin boundary. Nat. Commun. 12, 2139. https://doi.org/10.1038/s41467-021-22428-1.
Todoroki, M., Hara, K., Kudo, A., Sakata, T., 1995. Electrochemical reduction of high-pressure CO_2 at Pb, Hg and In electrodes in an aqueous $KHCO_3$ solution. J. Electroanal. Chem. 394, 199–203. https://doi.org/10.1016/0022-0728(95)04010-L.
Yaashikaa, P.R., Kumar, P.S., Varjani, S.J., Saravanan, A., 2019. A review on photochemical, biochemical and electrochemical transformation of CO_2 into value-added products. J. CO2 Util. 33, 131–147. https://doi.org/10.1016/j.jcou.2019.05.017.
Yang, S., Jiang, M., Wang, M., Wang, L., Song, X., Wang, Y., Tie, Z., Jin, Z., 2023. Rational design and synergistic effect of ultrafine Ag nanodots decorated fish-scale-like Zn nanoleaves for highly selective electrochemical CO_2 reduction. NanoResearch 16, 8910–8918. https://doi.org/10.1007/s12274-023-5596-z.
Yang, H., Kaczur, J.J., Sajjad, S.D., Masel, R.I., 2017. Electrochemical conversion of CO_2 to formic acid utilizing Sustainion™ membranes. J. CO2 Util. 20, 208–217. https://doi.org/10.1016/j.jcou.2017.04.011.
Zhang, H., Zeng, S., Jiang, C., Peng, K., Feng, J., Yuan, L., Li, X., Xu, F., Zhang, X., 2024. Efficient CO_2 electroreduction to CO facilitated by porous Ag (111) - dominant Ag nanofoams and cooperative ionic liquid electrolytes. ChemCatChem 16, e202400045. https://doi.org/10.1002/cctc.202400045.
Zong, S., Chen, A., Wisniewski, M., Macheli, L., Jewell, L.L., Hildebrandt, D., Liu, X., 2023. Effect of temperature and pressure on electrochemical CO_2 reduction: a mini review. Carbon Capture Sci. Technol. 8, 100133. https://doi.org/10.1016/j.ccst.2023.100133.